Available online at www.sciencedirect.com
SCIENCE DIRECT
Image and Vision Computing 24 (2006) 101–110
www.elsevier.com/locate/imavis

Adaptive fingerprint image enhancement with fingerprint image quality analysis

Eun-Kyung Yun, Sung-Bae Cho *

Department of Computer Science, Biometrics Engineering Research Centre, Yonsei University, 134 Shinchon-dong, Sudaemoon-ku, Seoul 120-749, South Korea

Received 7 November 2004; received in revised form 20 September 2005; accepted 24 September 2005

Abstract

Accurate minutiae extraction from fingerprint images is heavily dependent on the quality of the fingerprint images. In order to improve the performance of the system, much effort has been made on the image enhancement algorithms. If the preprocessing is adaptive to the fingerprint image characteristics in the image enhancement step, the performance gets to be more robust. In this paper, we propose an adaptive preprocessing method, which extracts five features from the fingerprint images, analyzes image quality with clustering method, and enhances the images according to their characteristics. Experimental results indicate that the proposed method improves the performance of the fingerprint identification significantly.

Keywords: Biometrics; Fingerprint identification; Fingerprint image quality; Image enhancement; Clustering

1. Introduction

Fingerprint identification is one of the most popular biometric technologies and is used in criminal investigations, commercial applications, and so on. The performance of a fingerprint image-matching algorithm depends heavily on the quality of the input fingerprint images [1]. It is very important to acquire good quality images but in practice a significant percentage of acquired images is of poor quality due to some environmental factors or user's body condition [2]. The poor quality images cause two problems: (1) many spurious minutiae may be created and (2) many genuine minutiae may be ignored. Therefore, an image enhancement algorithm is necessary to increase the performance of the minutiae extraction algorithm.

There are some on-going and past efforts in the investigation of fingerprint image quality. Hong et al. [3] modeled the ridge and valley patterns as a sine wave, and computed the amplitude and frequency to decide the quality of the fingerprint image. They evaluated the performance of their image enhancement algorithm using goodness index based on minutiae and verification performance. But they used quality check only for the performance evaluation of image enhancement algorithm. Ratha et al. [4] proposed a method for image quality estimation from wavelet scalar quantization (WSQ) images. This is only for WSQ compressed format and it is not the case for general fingerprint images. Lim et al. [5] developed local and global quality measures and estimated the quality and validity of fingerprint images. In addition, Bolle et al. [6] used the ratio of directional area to other non-directional area as a quality measure. Shen et al. [7] applied Gabor filter to image sub-blocks and concluded that a good quality block can be identified by the outputs of Gabor filter bank.

However, most of the quality checks have been used as a criterion, which determines image rejection, or a performance measurement of image enhancement algorithm. In this case, only images with room for improvement deliver to the system and are filtered uniformly. If the adaptive filtering is performed through appropriate analysis of image quality, images can be enhanced more effectively.

This paper proposes an adaptive preprocessing method to improve image quality appropriately. The preprocessing is performed after distinguishing the fingerprint image quality according to its characteristics. It is an adaptive filtering according to oily/dry/neutral images instead of uniform filtering. In the first stage, several features are extracted for image quality analysis and they go into the clustering module. Then, the adaptive preprocessing is applied to produce good quality images. We test the proposed method on NIST DB 4

* Corresponding author. Tel.: +82 2 2123 2720; fax: +82 2 365 2579.
E-mail addresses: ekfree@sclab.yonsei.ac.kr (E.-K. Yun), sbcho@cs.yonsei.ac.kr (S.-B. Cho).

0262-8856/$ - see front matter
doi:10.1016/j.imavis.2005.09.017

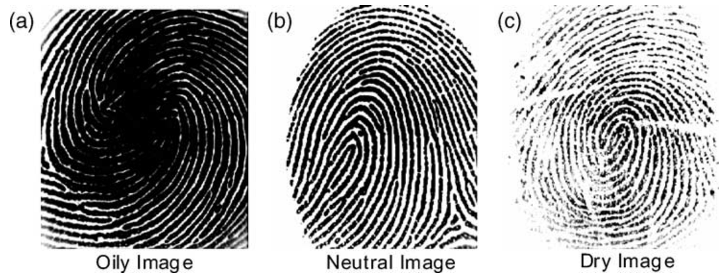

Fig. 1. Examples of fingerprint images.

and a private DB collected with careful consideration of image quality at Inha University.

2. Fingerprint identification

Fingerprint identification is the technology that distinguishes between the user oneself and others using the unique information in fingerprint. Fingerprints are the oldest biometric signs of identity. The inside surfaces of the hands from fingertips to wrist contain minute ridges of skin, with furrows between each ridge. The ridges have pores along their entire length that exude perspiration [8]. A fingerprint is believed to be unique to each person. Fingerprint identification begins based on this uniqueness. As shown in Fig. 1, a fingerprint image consists of ridges and valleys. A ridge is defined as a single curved segment and a valley is the region between two adjacent ridges. In general, black lines mean ridges and white lines mean valleys.

Fingerprint identification system consists of three main processes, which are acquisition, feature extraction, and matching as shown in Fig. 2 [9]. Firstly, the system obtains the digitalized fingerprint images using a sensor. Since in image acquisition external factors influence the image quality, preprocessing module has to enhance the image quality. After that, feature extraction is performed. The most common representation used in fingerprint identification is Galton features [10], which are called as minutiae. There are many different minutiae types that are extended from the Galton features. In most of the automatic identification systems, the minutiae are restricted to two types: ridge endings and ridge bifurcations [2]. Spurious minutiae need to be removed because most of the images may not always have well defined ridge structures and they have some spurious minutiae. Using these extracted minutiae, matching module is performed. At the matching stage, the templates from the claimant fingerprint are compared against that of the enrollee fingerprint.

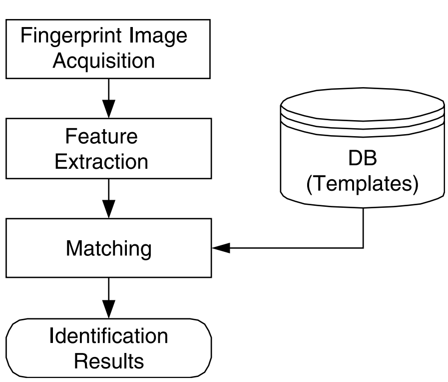

Fig. 2. Architecture of a fingerprint identification system.

As shown in Fig. 3, image quality and filtering algorithm affect the performance of minutiae extraction. The left image is original one and the right image shows the extracted minutiae after the conventional filtering. There are many endings since the original image has many broken ridges.

In general, the fingerprint image quality relies on the clearness of separated ridges by valleys and the uniformity of the separation. A fingerprint image changes in many ways because of the changes in environmental conditions such as temperature, humidity and pressure. The overall quality of the fingerprint depends greatly on the condition of the skin [2]. Dry skin tends to cause inconsistent contact of the finger ridges with the scanner's platen surface, causing broken ridges and many white pixels replacing ridge structure. To the contrary, the valleys on the oily skin tend to fill up with moisture, causing them to appear black in the image similar to ridge structure. Fig. 1 shows oily/neutral/dry images, respectively.

- Oily image: even though the separation of ridges and valleys is clear, some parts of valleys are filled up causing them to appear dark or adjacent ridges stand close to each other in many regions. Ridges tend to be very thick.
- Neutral image: in general, it has no special properties such as oily and dry. It does not have to be filtered.
- Dry image: the ridges are scratchy locally and there are many white pixels in the ridges.

In this paper, the preprocessing is subject to the image characteristics (oily/dry/neutral): for oily images, valleys are enhanced by dilating thin and disconnected ones (valley enhancement). For dry images, ridges are enhanced by extracting their centerlines and removing white pixels (ridge enhancement) [11]. Most of the fingerprint identification systems preprocess images without considering their characteristics as shown in Fig. 2. If the preprocessing suitable for their characteristics is performed, much better images can be obtained.

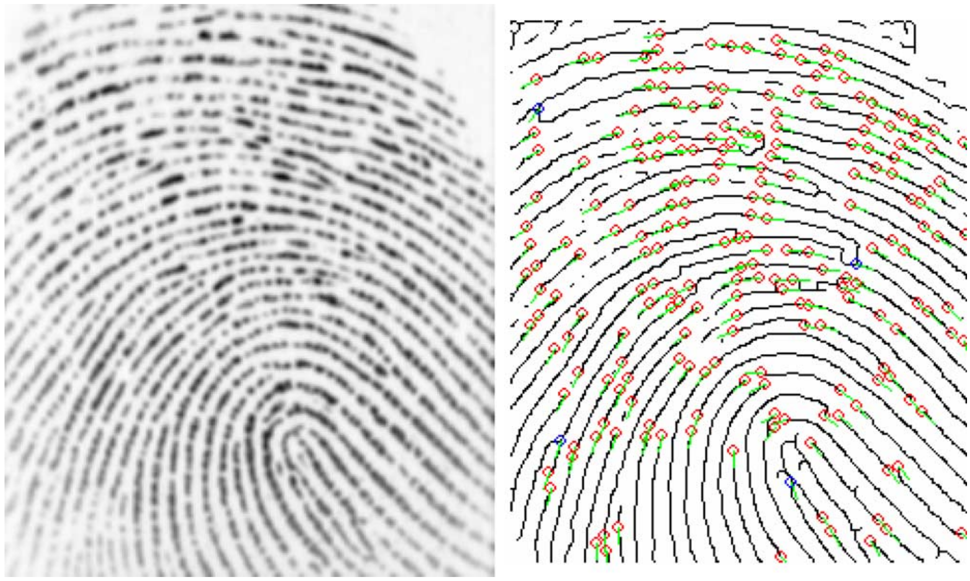

Fig. 3. Examples of minutiae extraction.

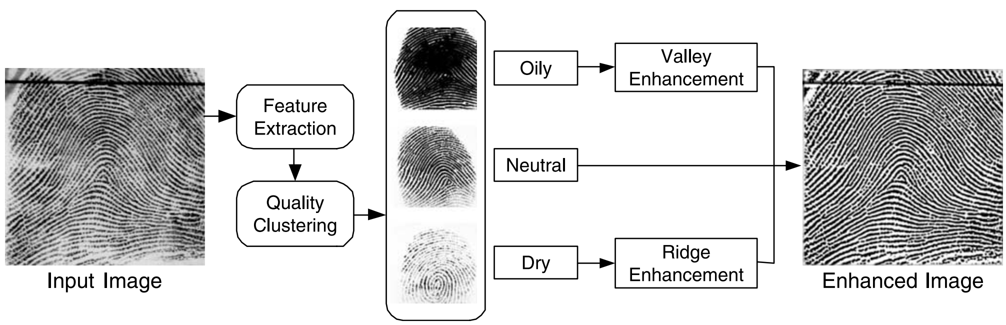

Fig. 4. System overview.

3. Adaptive image enhancement

Fig. 4 shows the whole system proposed in this paper. First, it extracts several features in fingerprint images for fingerprint image quality analysis. Features are extracted using orientation fields. Clustering algorithm groups fingerprint images with the features, and the images in each cluster are analyzed and preprocessed adaptively.

3.1. Feature extraction

In this paper, five features are used to grasp the image quality characteristics as shown in Table 1. The mean and variance of a gray-level fingerprint image are defined as follows.

$$\text{Mean} = \frac{1}{NM}\sum_{i=0}^{N-1}\sum_{j=0}^{M-1} I(i,j)$$

$$\text{Variance} = \frac{1}{NM}\sum_{i=0}^{N-1}\sum_{j=0}^{M-1} (I(i,j)-\text{Mean})^2$$

The mean of gray values indicates the overall gray level of the image and the variance shows the uniformity of the gray values. I(i,j) represents the intensity of the pixel at the i th row and j th column and the image I is defined as an N×M matrix.

Table 1
Features for image quality analysis

Feature	Definition	Purpose
Mean (M)	Mean of gray values	Measurement of whole gray level
Variance (V)	Variance of gray values	Uniformity of gray values
Block directional difference (B)	Mean of block directional difference	Distinctness between ridges and valleys
Ridge-valley thickness ratio (R)	Mean of ridge-valley thickness ratio	Measurement of ratio for ridge and valley thickness
Orientation change (O)	Using block orientation, summation of orientation change along each horizontal row and each vertical column of the image block	Measurement of ridge continuity

Fingerprint image is divided into a number of non-overlapping blocks and block directional difference is computed [10]. Using the 9×9 mask, slit sum S_i, i=1,…,8 is produced for center pixel C of the block.

$$S_i = \sum_{i=1}^{8} P_{ij} \text{ block directional difference} = \mathrm{Sum}(|S_{\max} - S_{\min}|)$$

where $S_{max}=\mathrm{Max}\{S_i,\ i=1,2,\ldots,8\}$ and $S_{min}=\mathrm{Min}\{S_i,\ i=1,2,\ldots,8\}$.

P_{ij} denotes the gray-level value of the j-th pixel in the direction i. S_{max} and S_{min} appear in each valley (white) pixel and in each ridge (black) pixel, respectively. Therefore, the directional difference of image block has a large value for good quality image blocks. In other words, ridge structures are characterized as well separated. For bad quality image blocks, the directional difference of image block has a small value. Namely, ridge and valley are not distinguished in each other.

The ratio for ridge thickness to valley thickness is computed in each block [5]. Ridge thickness and valley thickness are obtained using gray level values for one image block in the direction normal to ridge flow. After that, the ratio of each block is computed and average value of the ratio is obtained over the whole image.

Orientation change is obtained by accumulating block orientation along each horizontal row and each vertical column of the image block. Orientation computation is as follows [12].

(1) Divide I into blocks of size ω×ω.
(2) Compute the gradients $(_x(i,j)$ and $(_y(i,j)$ at each pixel (i,j) with the Sobel operator.
(3) Estimate the local orientation of each block centered at pixel (i,j) using the following equations [13]:

$$V_x(i,j) = \sum_{u=i-\frac{w}{2}}^{i+\frac{w}{2}} \sum_{v=j-\frac{w}{2}}^{j+\frac{w}{2}} 2\partial_x(u,v)\partial_y(u,v)$$

$$V_y(i,j) = \sum_{u=i-\frac{w}{2}}^{i+\frac{w}{2}} \sum_{v=j-\frac{w}{2}}^{j+\frac{w}{2}} (\partial_x^2(u,v)\partial_y^2(u,v))$$

$$\theta(i,j) = \frac{1}{2}\tan^{-1}\left(\frac{V_y(i,j)}{V_x(i,j)}\right)$$

where θ(i,j) is the least square estimate of the local ridge orientation at the block centered at pixel (i,j). It represents the direction that is orthogonal to the direction of the Fourier spectrum of the ω×ω window. In this paper, we set ω=16 and feature values are normalized between 0 and 1.

3.2. Image quality clustering

As mentioned before, fingerprint image quality is divided into three classes, dry/neutral/oily. In this paper, we cluster images according to their characteristics using five features defined before. Fingerprint images are clustered by Ward's clustering algorithm [14].

Ward's algorithm, which is one of the hierarchical clustering methods, initially assigns an independent cluster to each sample. Then it seeks the most similar pairs of clusters and merges them into one cluster. This process is repeated until all of the initial clusters are merged into a single cluster. Ward's method has been widely applied to cluster analysis since it can visualize hierarchical structure of clusters with a dendrogram [15]. It measures the similarity using the sum of squares within a cluster. Let $X_{ld}=(x_{ld}^1, x_{ld}^2, \ldots, x_{ld}^k)$ and n_l denote the value of the d-th example with k attributes in a cluster l and the number of examples in l. Then the sum of squares of cluster l, S_l, is defined as:

$$S_l = \sum_{i=1}^{n_l} \sum_{j=1}^{k} (x_{ld}^j - \bar{x}_l^j)^2$$

where $\bar{x}_l^j$ is defined as:

$$\bar{x}_l^j = \frac{1}{n_l} \sum_{i=1}^{n_l} x_{li}^j$$

Let us consider the integration of cluster l and cluster m into cluster lm. The two clusters, l and m, will be integrated when ΔS_{lm} is minimum with respect to all the clusters. ΔS_{lm} is obtained as:

$$\Delta S_{lm} = \frac{n_l n_m}{n_l + n_m} \sum_{j=1}^{k} (\bar{x}_l^j - \bar{x}_m^j)^2$$

Then, the sum of squares of cluster lm is obtained as $S_{lm}=S_l+S_m+\Delta S_{lm}$.

In this paper, image quality clustering tests on NIST DB 4 using five features described before. A total 2000 (a half of NIST DB) five-dimensional patterns are used as input vectors of clustering algorithm. To determine the proper number of clusters, Mojena's cut-off value is used [15].

$$\text{Mojena's value} = \bar{h} + \alpha s_h$$

where $\bar{h}$ is the average of dendrogram heights for all N-1 clusters and s_h is the unbiased standard deviation of the heights. α is a specified constant and according to Milligan and Cooper [16], the best overall performance of Mojena's rule occurs when the values of α is 1.25. For that reason, we set α=1.25 as the number of clusters.

3.3. Adaptive preprocessing

Smoothing is one of the conventional filtering methods [10]. It can remove the white pixels of ridges in case of dry images; however, it also removes necessary ridges that are thinner than neighbor ridges. Similarly, in case of oily images, it removes necessary valleys that are very thin while it removes black noises of valleys. As shown in Fig. 5, (a) and (c) are dry and oily images, respectively, and (b) and (d) are the results with smoothing uniformly. In smoothing on the dry image, some

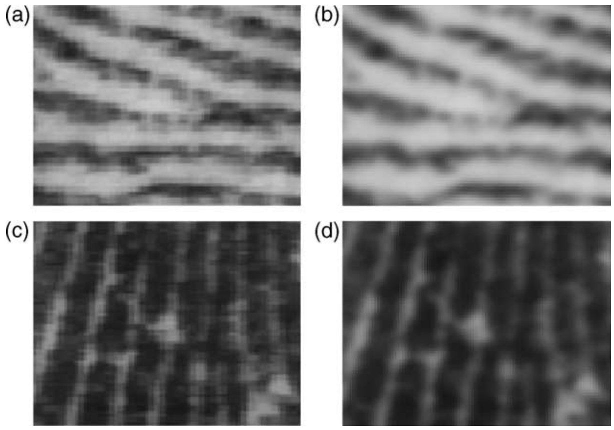

Fig. 5. Results of conventional filtering.

white noises of ridges are eliminated but very thin ridges grow dim and the outlines are not clear.

Therefore, adaptive filtering with classifying image characteristics is better than uniform filtering. Fig. 6 shows a preprocessing method appropriate to image quality characteristics [11]. That is, ridges are enhanced in dry images and valleys are enhanced in oily images.

In this paper, preprocessing is performed based on binary images, because gray level images have more information than binary images even though the processing time in gray ones is longer than that in binary ones. Adaptive filtering procedure is defined as follows:

(1) Ridge enhancement of dry images: this extracts center lines of ridges and removes white pixels in ridges using this center-lined image. It also maintains the structure of the fingerprint.
   A. Smoothing: smoothing is applied to the original image to reduce noises.
   B. Thinning: a thinned image is obtained for extraction of ridge structures.
   C. Dilation: a thinned image is dilated.
   D. Extracting the union of black pixels in an original image and the image in C: white pixels in the ridges are removed. In this way, the ridge-enhanced image is obtained.
(2) Valley enhancement of oily images: it is more complicated than ridge enhancement. It needs to detect regions where valleys are thin and disconnected. For this, thinning function extracts only the ridges thinner than a threshold. It means that the ridges wider than a threshold are eliminated.
   A. Smoothing: it eliminates thin and disconnected valleys.
   B. Thinning: thinned image using the threshold is obtained for extraction of ridge structures.
   C. Dilation: dilated image is obtained and it contains the regions where ridges are sufficiently separated as black and the regions where ridges touch one another as white.

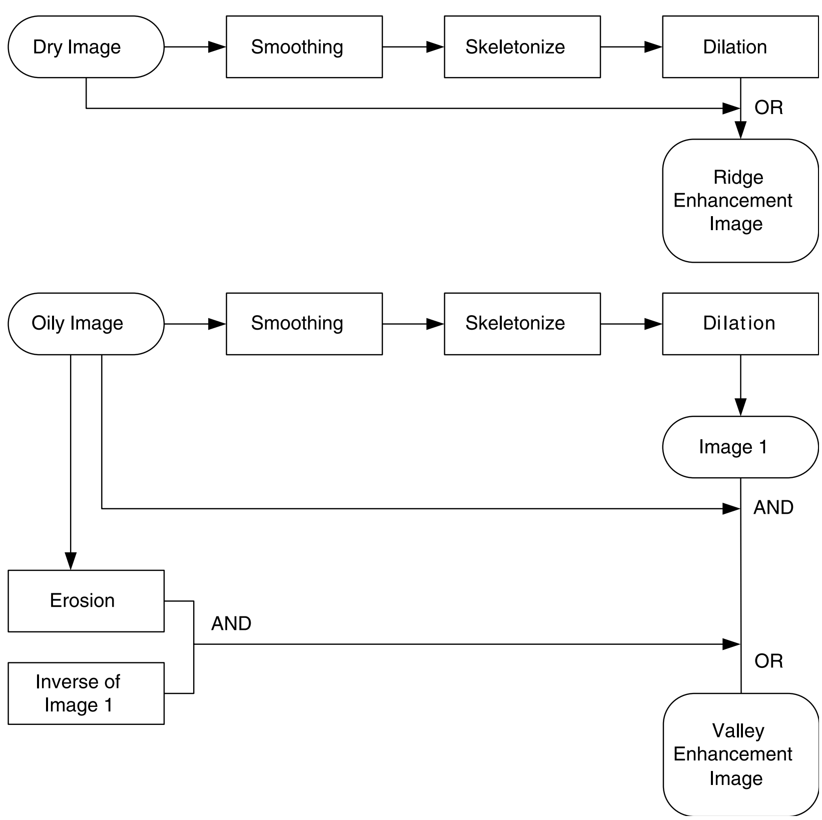

Fig. 6. Preprocessing appropriate to image characteristics.

D. Composition of black pixels in the original image and in the image obtained in C: it detects the ridges whose thickness is wider than a threshold.
E. Composition of black pixels in the erosion of an original image and an inverse image of an image in C.
F. Extracting the union of black pixels of the images in D and E: in this way, the valleyenhanced image is obtained.

4. Experimental results

The proposed method is verified with the NIST DB 4 (DB1) [17] and the highly controlled fingerprint DB at Inha University (DB2) [18]. DB1 consists of 4000 fingerprint images (image size is 512×480) from 2000 fingers. Each finger has two impressions. In DB2, the size of images is 248×292. Both of DB1 and DB2 are gray-level images. DB2 is used to check whether minutiae are extracted correctly or not. We use the first 2000 fingerprint images in DB1 for clustering and the remaining 2000 images for adaptive filtering using the rules obtained from the clustering results.

Fingerprint image characteristics are analyzed using the Ward's clustering results (Fig. 7). Thirty clusters in a high rank appear in the dendrogram and according to Mojena's rule the proper number of clusters is 5. Fig. 8 shows feature distribution in each cluster. Cluster 4 is assigned as dry, cluster 5 is oily and the remaining three clusters are neutral.

As a result, clustering made total 23 rules and Fig. 9 shows the essential rules. It indicates that in oily images, ridges tend to be thicker than valleys and in dry images the ratio of ridge valley thickness and mean are different from other clusters. In addition, the important factor of each feature is obtained by using the feature frequency in the rules. As shown in Table 2, the ridge-valley thickness ratio is the most important feature. It is also the judgment criterion for human to detect the fingerprint image characteristics.

Fig. 10 shows some representative examples of each cluster: (a)–(c) are oily images, (d)–(f) are neutral ones and (g)–(i) are dry ones. It means that images with similar features are grouped into the same clusters. Using these clustering results, adaptive filtering and conventional filtering are performed. As shown in Fig. 11, adaptively filtered images have better quality than conventionally filtered images.

The image quality is measured in two different ways for quantitative analysis. First, block directional difference is used for quality check [17]. When the image quality is checked manually, we determine the image quality using the clearly separated ridges by valleys [5]. Hence, the block directional difference has a large value for good quality images. As shown in Fig. 12, the adaptive preprocessing is better than the uniform conventional filtering. The average values of the block directional difference with the adaptive enhancement are larger than those with the conventional filtering.

Second, the quality is measured with extracted minutiae. Image quality is assessed by comparing the minutiae set identified by human expert with that detected by minutiae extraction algorithm in an input fingerprint image. The larger the value of quality index, the better the minutiae extraction algorithm. Quality index is defined as follows:

$$\text{Quality index} = \frac{c}{c+f+u}$$

where c is the number of correctly detected minutiae, f is the

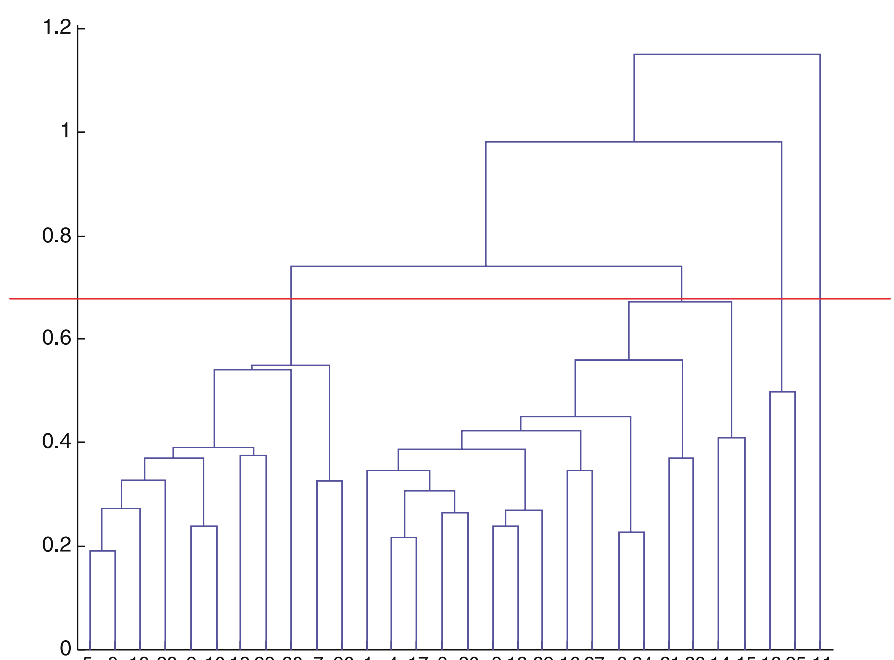

Fig. 7. Fingerprint image clustering results using Ward's algorithm.

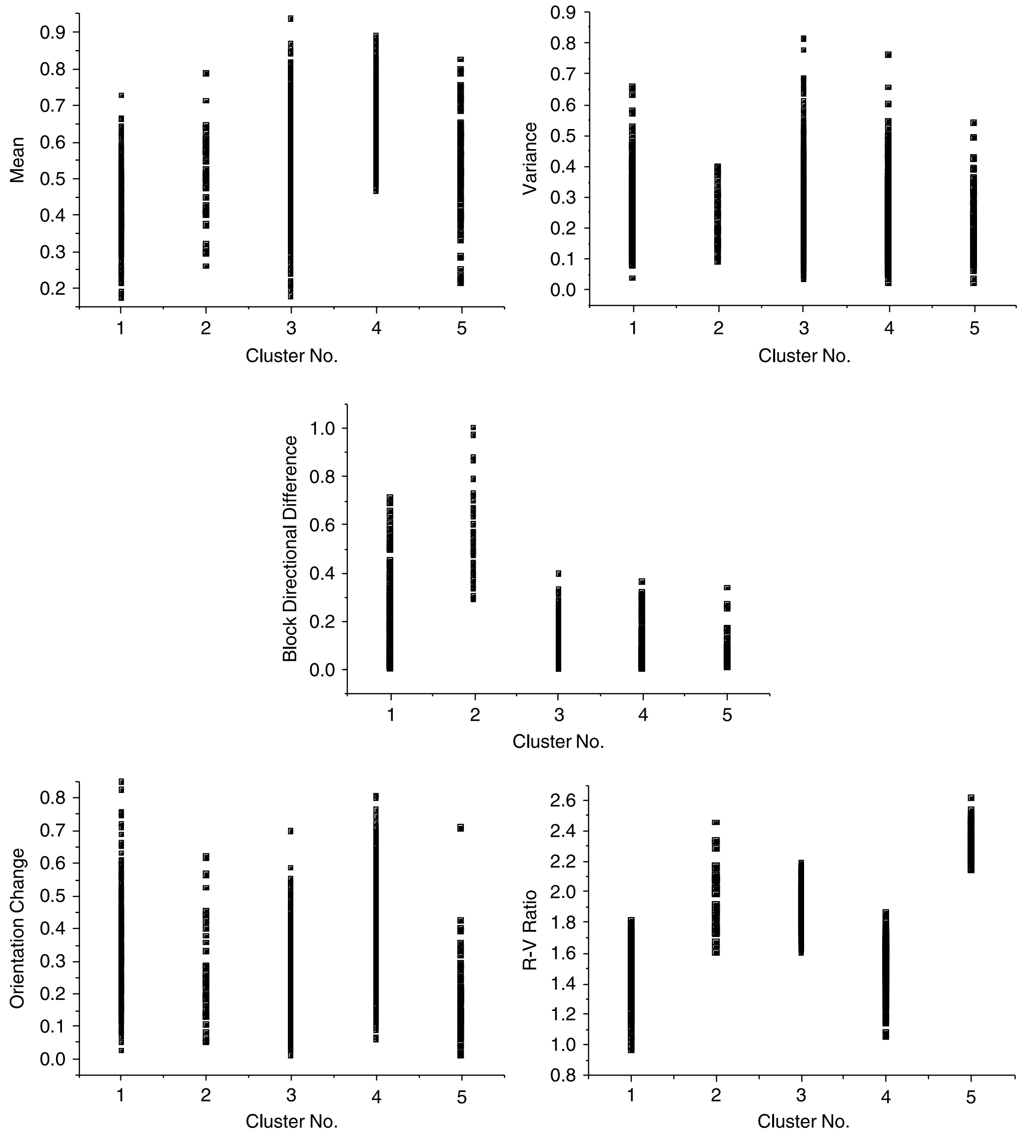

Fig. 8. Feature distribution for each cluster.

number of falsely detected minutiae, and u is the number of undetected minutiae.

We use the 50 typical poor fingerprint images from DB2 to measure the filtering performance using extracted minutiae. First, we compute the quality index of the extracted minutiae with the conventional filtering and then the quality index of the extracted minutiae is computed with the adaptive filtering. Table 3 shows the quality index values of 50 typical images and the mean and variance of quality index values for all images. The quality index values with the adaptive enhancement are larger than those with the conventional filtering. Thus, it means that the adaptive preprocessing method improves the quality of the fingerprint images, which improves the accuracy of the extracted minutiae. To determine if there is a reliable difference between two means, we conduct a paired t-test. As shown in Table 4, t-value (5.49) and p-value (<0.0001) indicate that the difference between the two means is statistically very

```
IF ((B < 0.041) and (R >= 2.17))
   THEN  Oily Cluster
ELSE IF ((V <0.24) and (2.14 <= R < 2.17) and (B < 0.29))
   THEN  Oily Cluster
ELSE IF ((V < 0.39) and (O >= 0.21) and (B < 0.33) and (R < 1.73))
   THEN  Dry Cluster
ELSE IF ((M >= 0.54) and (B < 0.12) and (V >= 0.39) and (O >= 0.21) and (R < 1.73))
   THEN  Dry Cluster
ELSE  Neutral Cluster
```

Fig. 9. Rules obtained by clustering.

Table 2
Important factor of each feature

Feature	Important factor
Mean (M)	0.67
Variance (V)	0.20
Block directional difference (B)	0.37
Orientation change (O)	0.36
Ridge-valley thickness ratio (R)	1.00

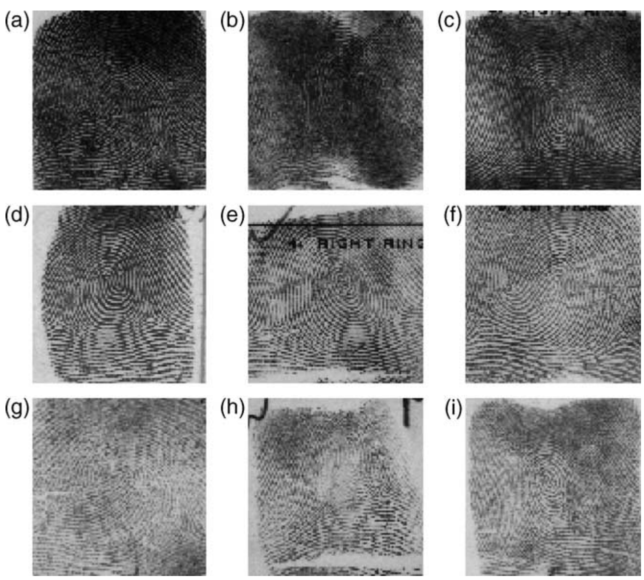

Fig. 10. Examples of clustering results: (a)–(c) are oily images, (d)–(f) are neutral ones and (g)–(i) are dry ones.

significant. That is, the quality difference between the conventional filtered images and adaptive filtered images is very significant in 99% confidence level.

Figs. 13 and 14 show some examples of enhanced images through the adaptive preprocessing. Fig. 13 shows the minutiae extracted in dry images with conventional filtering and adaptive filtering: (a) and (c) are with conventional filtering,

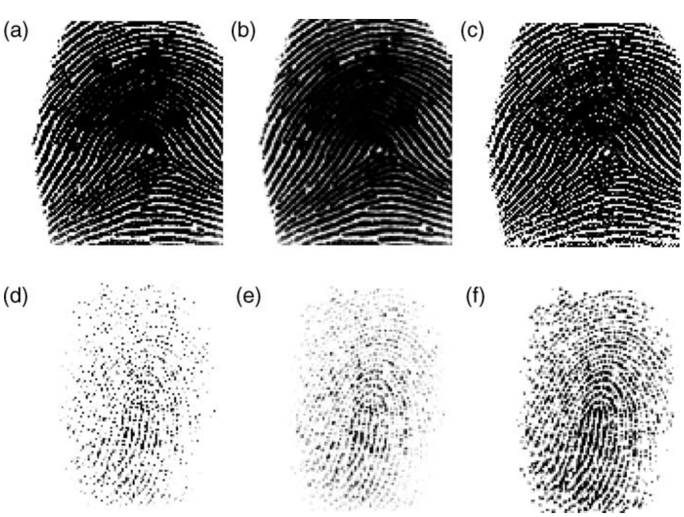

Fig. 11. Examples of enhancement results.

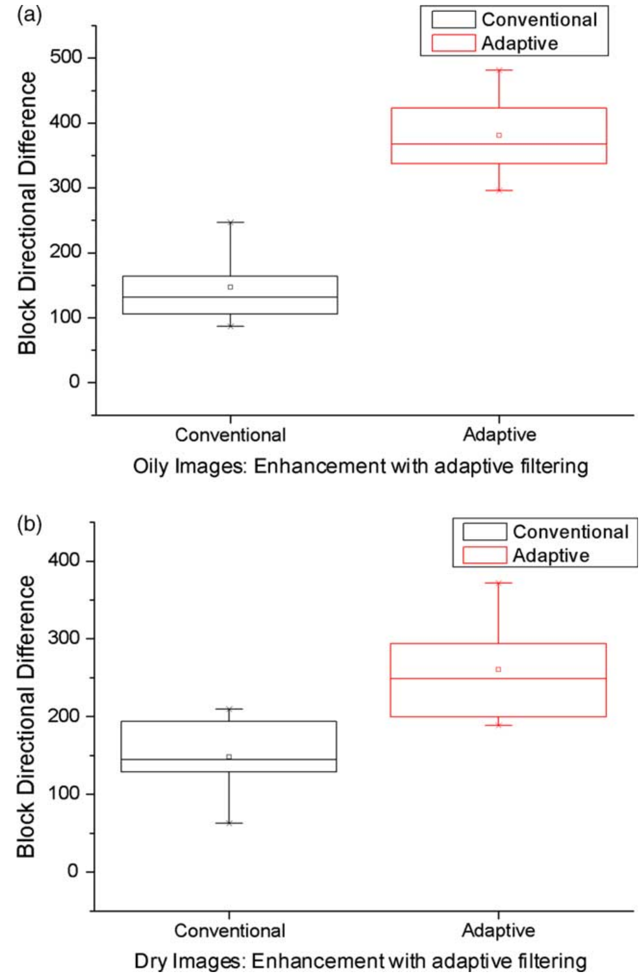

Fig. 12. Enhancement results with block directional difference.

(b) and (d) are with ridge enhancement filtering. While (a) and (c) have some falsely detected minutiae, endings, (b) and (d) have the correctly detected minutiae, bifurcations. Fig. 14 shows the minutiae extracted in oily images. While (a) and (c) with conventional filtering have falsely detected minutiae, bifurcations, or ridges connected, (b) and (d) with valley enhancement have correctly detected minutiae.

In order to incorporate the proposed preprocessing method into an online system, the whole process should be finished within a few seconds. Table 5 shows the time for each feature extraction and preprocessing.

Finally, we test the identification performance with this adaptive image enhancement. The performance of a biometric system can be shown as receiver operating characteristic (ROC) curves, showing the genuine accept rate (1-FRR (false reject rate)) against the false accept rate at different thresholds on the matching score. Fig. 15 shows the performance of the proposed method. As can be seen in this graph, the proposed method outperforms the conventional method over a little range of FAR values. For example, at a 10% FAR, the proposed method gives a genuine accept rate of 96% while the conventional method gives a genuine accept rate of 92%.

Table 3
The quality index values of fingerprint images: 50 typical images and the mean and variance

Image #	Conventional filtering	Adaptive filtering	Image #	Conventional filtering	Adaptive filtering
1	0.16	0.37	27	0.11	0.18
2	0.25	0.27	28	0.08	0.14
3	0.0	0.25	29	0.03	0.06
4	0.0	0.18	30	0.24	0.32
5	0.07	0.1	31	0.07	0.13
6	0.0	0.0	32	0.0	0.22
7	0.0	0.24	33	*0.34*	*0.32*
8	0.0	0.06	34	0.35	0.4
9	0.12	0.14	35	0.06	0.22
10	0.07	0.1	36	0.27	0.37
11	0.17	0.2	37	0.38	0.42
12	*0.09*	*0.07*	38	0.31	0.41
13	0.15	0.22	39	*0.33*	*0.22*
14	*0.16*	*0.14*	40	0.33	0.56
15	0.23	0.4	41	0.27	0.41
16	*0.21*	0.2	42	0.22	0.31
17	*0.22*	*0.16*	43	0.22	0.45
18	0.05	0.1	44	0.16	0.18
19	0.12	0.19	45	0.11	0.18
20	0.06	0.07	46	0.32	0.41
21	*0.22*	*0.1*	47	0.02	0.11
22	0.06	0.2	48	0.08	0.32
23	0.02	0.05	49	0.11	0.12
24	0.08	0.08	50	0.3	0.5
25	*0.28*	*0.25*	Mean	0.1512	0.2226
26	*0.06*	0.03	Variance	0.0130	0.0183

Table 4
Results of paired t-test

Mean	Standard deviation	t-Value	Pr > |t|
0.0714	0.013	5.49	< 0.0001

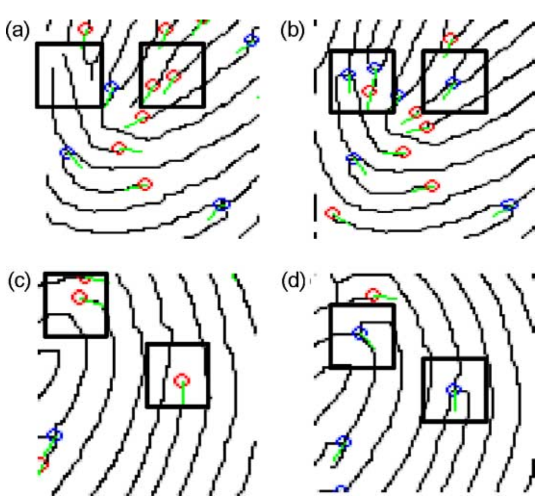

Fig. 13. Dry image examples of minutiae extraction with conventional/adaptive filtering: (a) and (c) show the extracted minutiae with the conventional filtering, (b) and (d) show the extracted minutiae with ridge enhancement.

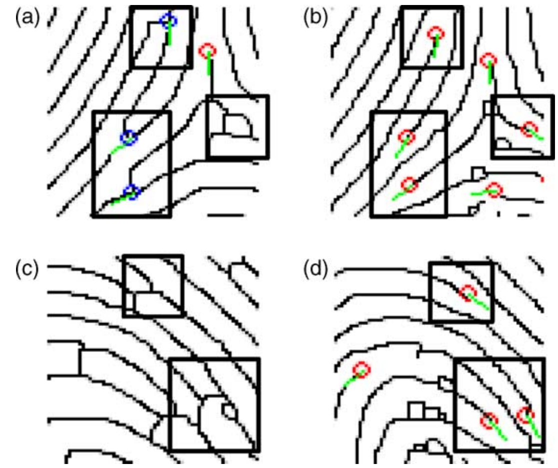

Fig. 14. Oily image examples of minutiae extraction with conventional/adaptive filtering: (a) and (c) show the extracted minutiae with the conventional filtering, (b) and (d) show the extracted minutiae with valley enhancement.

Table 5
The time for the adaptive preprocessing (seconds) on Pentium 2 GHz PC

M & V	B	O	R	Preprocessing	Total
0.001	0.141	0.063	0.047	0.301	0.553

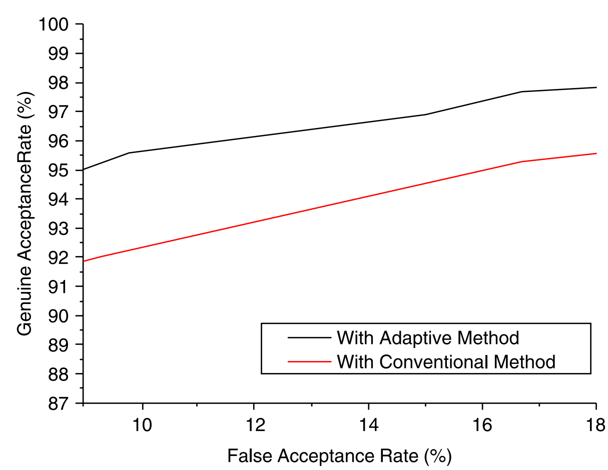

Fig. 15. ROC curve comparing the performance of the proposed method with the conventional method.

5. Conclusions

The performance of fingerprint identification system relies critically on the image quality. Hence, good quality images make the system performance more robust. However, it is always very difficult to obtain good quality images in practical use. To overcome this problem, image enhancement step is required. Most of the enhancement algorithms are applied to images equally without considering the image characteristics. Even though quality check is performed, it is not for quality analysis but for the performance evaluation of image enhancement algorithms or for checking whether an image is improved or not.

In this paper, we have proposed an adaptive image enhancement method for fingerprint identification system. It is performed through image quality characteristics analysis. The performance of the proposed method was evaluated using the block directional difference and the quality index of the extracted minutiae. Experimental results show that the proposed method is able to improve both quality measurements. In terms of the identification performance, the proposed method is better than the conventional one. Further works are going on to develop image characteristic factors for the identification system in real worlds.

Acknowledgements

This work was supported by the Korea Science and Engineering Foundation (KOSEF) through the Biometrics Engineering Research.

References

[1] N.K. Ratha, K. Karu, S. Chen, A.K. Jain, A real-time matching system for large fingerprint databases, IEEE Transaction on Pattern Analysis and Machine Intelligence 18 (8) (1996) 799–813.
[2] L.C. Jain, U. Halici, I. Hayashi, S.B. Lee, S. Tsutsui, Intelligent Biometric Techniques in Fingerprint and Face Recognition, CRC Press, 1999.
[3] L. Hong, Y. Wan, A.K. Jain, Fingerprint image enhancement: algorithm and performance evaluation, IEEE Transaction on Pattern Analysis and Machine Intelligence 20 (8) (1998) 777–789.
[4] N.K. Ratha, R.M. Bolle, Fingerprint Image Quality Estimation, IBM Computer Science Research Report RC 21622, 1999
[5] E. Lim, X. Jiang, W. Yau, Fingerprint quality and validity analysis, IEEE International Conference on Image Processing (ICIP 2002), 1 2002 pp. 22–25.
[6] R. Bolle, S. Pankanti, Y.-S. Yao, System and Method for Determining the Quality of Fingerprint Images, US Patent Number US 596356, 1999
[7] L.L. Shen, A. Kot, W.M. Koo, Quality measures of fingerprint images. The 3rd International Conference Audio- and Video-based Biometric Person Authentication (AVBPA 2001), 2001, pp. 182–271.
[8] H.C. Lee, R.E. Gaensslen, Advances in Fingerprint Technology, CRC Press, 2001.
[9] A.K. Jain, S. Pankanti, S. Prabhakar, A. Ross, Recent advances in fingerprint verification, 3rd International Conference on Audio- and Video-Based Person Authentication, 2001, pp. 182–191.
[10] F. Galton, Finger Prints, Macmillan, London, 1892.
[11] N. Ikeda, M. Nakanishi, K. Fujii, T. Hatano, S. Shigematsu, T. Adachi, Y. Okazaki, H. Kyuragi, Fingerprint image enhancement by pixel-parallel processing, 16th International Conference on Pattern Recognition, 2002, pp. 752–755.
[12] K. Karu, A. Jain, Fingerprint classification, Pattern Recognition 29 (3) (1996) 389–404.
[13] A. Rao, A Taxonomy for Texture Description and Identification, Springer, New York, NY, 1990.
[14] J.H. Ward, Hierarchical grouping to optimize an objective function, Journal of the American Statistical Association 58 (301) (1963) 236–244.
[15] R. Mojena, Hierarchical grouping methods and stopping rules: an evaluation, Computer Journal 20 (1977) 353–363.
[16] G.W. Milligan, K.C. Cooper, An examination of procedures for determining the number of clusters in a data set, Psychometrika 50 (1985) 159–179.
[17] C.I. Watson, C.L. Wilson, NIST special database 4, fingerprint database. US nat'l, Inst. of Standards and Technology, 1992.
[18] H. Kang, B. Lee, H. Kim, D. Shin, J. Kim, A study on performance evaluation of fingerprint sensors, The 4rd International Conference Audio- and Video-based Biometric Person Authentication (AVBPA 2003), 2003, pp. 574–583.

Eun-Kyung Yun received the BS and MS degree in computer science from Yonsei University, Seoul, Korea, in 2002 and 2004, respectively. Now, she works at Samsung Electronics in Korea. Her research interests include pattern recognition, biometrics, and intelligent systems.

Sung-Bae Cho (Member, IEEE) received the BS degree in computer science from Yonsei University, Seoul, Korea, in 1988 and the MS and PhD degrees in computer science from Korea Advanced Institute of Science and Technology (KAIST), Taejeon, Korea, in 1990 and 1993, respectively. From 1991 to 1993, he worked as a Member of the Research Staff at the Center for Artificial Intelligence Research at KAIST. From 1993 to 1995, he was an Invited Researcher of Human Information Processing Research Laboratories at ATR (Advanced Telecommunications Research) Institute, Kyoto, Japan. In 1998, he was a Visiting Scholar at University of New South Wales, Canberra, Australia. Since 1995, he has been a Professor in the Department of Computer Science, Yonsei University. His research interests include neural networks, pattern recognition, intelligent man-machine interfaces, evolutionary computation, and artificial life. Dr Cho is a Member of the Korea Information Science Society, INNS, the IEEE Computer Society, and the IEEE Systems, Man and Cybernetics Society. He was awarded outstanding paper prizes from the IEEE Korea Section in 1989 and 1992, and another one from the Korea Information Science Society in 1990. In 1993, he also received the Richard E. Merwin prize from the IEEE Computer Society. In 1994, he was listed in Who's Who in Pattern Recognition from the International Association for Pattern Recognition and received the best paper awards at International Conference on Soft Computing in 1996 and 1998. In 1998, he received the best paper award at World Automation Congress. He was listed in Marquis Who's Who in Science and Engineering in 2000 and in Marquis Who's Who in the World in 2001.